the plant journal

SEB SOCIETY FOR EXPERIMENTAL BIOLOGY

The Plant Journal (2022) **111,** 1368–1382 doi: 10.1111/tpj.15894

Wheat photosystem II heat tolerance: evidence for genotype-by-environment interactions

Onoriode Coast[1,2,3,*], Bradley C. Posch[1], Bethany G. Rognoni[4,*], Helen Bramley[5], Oorbessy Gaju[1,6], John Mackenzie[1], Claire Pickles[7], Alison M. Kelly[4,8], Meiqin Lu[9], Yong-Ling Ruan[10], Richard Trethowan[5,11] and Owen K. Atkin[1]

[1]*ARC Centre of Excellence in Plant Energy Biology, Research School of Biology, The Australian National University, Canberra, ACT 2601, Australia,*

[2]*Natural Resources Institute, University of Greenwich, Central Avenue, Chatham Maritime, Kent ME4 4TB, UK,*

[3]*School of Environmental and Rural Sciences, Faculty of Science Agriculture Business and Law, University of New England, Armidale, NSW 2351, Australia,*

[4]*Department of Agriculture and Fisheries, Leslie Research Facility, Toowoomba, QLD 4350, Australia,*

[5]*School of Life and Environmental Sciences, Plant Breeding Institute, Sydney Institute of Agriculture, The University of Sydney, Narrabri, NSW 2390, Australia,*

[6]*Lincoln Institute of Agri-Food Technology, University of Lincoln, Riseholme Park, Lincoln, Lincolnshire LN2 2LG, UK,*

[7]*Birchip Cropping Group, 73 Cumming Avenue, Birchip, VIC 3483, Australia,*

[8]*Queensland Alliance for Agriculture and Food Innovation, The University of Queensland, Toowoomba, QLD 4350, Australia,*

[9]*Australian Grain Technologies, 12656 Newell Highway, Narrabri, NSW 2390, Australia,*

[10]*Division of Plant Sciences, Research School of Biology, The Australian National University, Canberra, ACT 2601, Australia, and*

[11]*School of Life and Environmental Sciences, Plant Breeding Institute, Sydney Institute of Agriculture, The University of Sydney, Cobbitty, NSW 2570, Australia*

Received 7 March 2022; revised 24 June 2022; accepted 28 June 2022; published online 4 July 2022.
*For correspondence (e-mail: ocoast@une.edu.au; bethany.rognoni@daf.qld.gov.au).

SUMMARY

High temperature stress inhibits photosynthesis and threatens wheat production. One measure of photosynthetic heat tolerance is T_{crit} – the critical temperature at which incipient damage to photosystem II (PSII) occurs. This trait could be improved in wheat by exploiting genetic variation and genotype-by-environment interactions (GEI). Flag leaf T_{crit} of 54 wheat genotypes was evaluated in 12 thermal environments over 3 years in Australia, and analysed using linear mixed models to assess GEI effects. Nine of the 12 environments had significant genetic effects and highly variable broad-sense heritability (H^2 ranged from 0.15 to 0.75). T_{crit} GEI was variable, with 55.6% of the genetic variance across environments accounted for by the factor analytic model. Mean daily growth temperature in the month preceding anthesis was the most influential environmental driver of T_{crit} GEI, suggesting biochemical, physiological and structural adjustments to temperature requiring different durations to manifest. These changes help protect or repair PSII upon exposure to heat stress, and may improve carbon assimilation under high temperature. To support breeding efforts to improve wheat performance under high temperature, we identified genotypes superior to commercial cultivars commonly grown by farmers, and demonstrated potential for developing genotypes with greater photosynthetic heat tolerance.

Keywords: chlorophyll fluorescence, factor analytic models, heat stress, multi-environment trial, photosynthesis, photosynthetic thermal tolerance, *Triticum aestivum*.

INTRODUCTION

Photosynthesis is an important determinant of plant biomass and crop yield. High temperature (warmer nights and days, and heatwaves) can inhibit photosynthesis, resulting in reduced crop yield. Global warming has been correlated with worldwide wheat (*Triticum aestivum* L.) yield losses (Asseng et al., 2015, 2017; Zhao et al., 2017). Additionally, models have predicted wheat yield decreases of up to 6% per 1°C warming (Zhao et al., 2017). In Australia, wheat yield loss due to high temperature is estimated to cost $1.1

billion per annum (GRDC, 2018) and, considering Australia accounts for approximately 11% of global wheat exports (ABARES, 2021; Qureshi et al., 2013), these losses can potentially affect global food security. To better adapt Australian wheat production to warming it is crucial to identify genotypes with traits – such as photosystem II (PSII) heat tolerance – that confer heat tolerance and are easy to phenotype so that these can be incorporated into breeding programmes.

Heat tolerance of PSII is often inferred from measuring leaf chlorophyll-*a* fluorescence (Geange et al., 2020) – light emitted by chloroplasts due to changes in PSII complexes embedded within the thylakoid membrane (Maxwell & Johnson, 2000). A commonly used chlorophyll-*a* fluorescence parameter is the temperature at which the maximum quantum efficiency of PSII (F_V/F_M) – defined as the ratio of variable fluorescence (difference between the basal chlorophyll-*a* fluorescence, F_0, and maximum chlorophyll-*a* fluorescence, F_M) to maximum fluorescence – is reduced by 50% (i.e. T_{50} of F_V/F_M). F_V/F_M has been applied in mass screening of wheat cultivars for high temperature tolerance (Azam et al., 2015; Sharma et al., 2012, 2017). Another chlorophyll-*a* fluorescence measure for assessing PSII heat tolerance is the critical temperature of PSII function (T_{crit} of F_0, henceforth T_{crit}). T_{crit} is determined as the temperature at which F_0 rises abruptly as leaves are warmed, and signifies the onset of damage to PSII (Berry & Bjorkman, 1980; Schreiber & Berry, 1977). T_{crit} is widely used in ecological studies (Hüve et al., 2006; Knight & Ackerly, 2002; O'Sullivan et al., 2017; Zhu et al., 2018) and recently applied in agricultural studies (Posch et al., 2022). As well as being a robust measure of thermal damage to PSII function similar to T_{50} of F_V/F_M (Lin, 2012; Marias et al., 2017; Perez & Feeley, 2020), the recent development of high-throughput phenotyping tools for measuring T_{crit} (Arnold et al., 2021; Posch et al., 2022) has made it possible to include T_{crit} measurements in the large-scale trials typical of breeding programmes.

T_{crit} responds to changes in growth environment conditions and varies among species (Lancaster & Humphreys, 2020; O'Sullivan et al., 2017; Rekika et al., 1997; Zhu et al., 2018). Genetic gains in breeding for high temperature tolerance could be improved with information from experiments that account for how T_{crit} is affected by both genotype and environment, as well as their interaction. Genotype-by-environment interactions (GEI) characterise the differential response of genotypes to changes in the environment, and are a common impediment to the selection of superior genotypes. GEI is the primary reason why breeders conduct multi-environment trials (METs; a set of connected trials across multiple years and environments). Incorporating measurements of T_{crit} in METs can provide useful information on yield stability and adaptability of genotypes to defined environment types (or the target population of environments; Comstock, 1977). The designs of METs are often highly unbalanced, and analysis of these data using traditional methods such as ANOVA are typically inadequate (Smith et al., 2015). A more flexible and superior approach for MET analysis uses factor analytic (FA) models (Smith et al., 2001). By combining FA models with graphical tools, such as latent regression plots and heatmaps of the estimated genetic correlation matrix across environments (Smith et al., 2015; Smith & Cullis, 2018), GEI can be explored and superior genotypes identified (i.e. those with high performance and stability across the target population of environments). Additionally, loadings from FA models can be linked with environmental covariates to identify important environmental drivers of T_{crit} GEI. This approach has been used to explore trends in species performance across environments in both plant and animal studies, including for wheat yield (Trethowan et al., 2018), lodging tolerance in spring wheat (Dreccer et al., 2020), sorghum [*Sorghum bicolor* (L.) Moench] biomass under drought (Oliveira et al., 2020), and body weight at harvest of the farmed fish species rainbow trout (*Onchorynchus mykiss*; Sae-Lim et al., 2014).

We conducted METs comprising 12 thermal environments (across 3 years) in Australia with a total of 54 wheat genotypes (Table S1), and assessed the GEI effect on PSII heat tolerance in wheat. These wheat genotypes were chosen from an extensive national wheat breeding programme for their diversity in heat tolerance. The genotypes included an elite subset of heat-tolerant, semi-dwarf germplasm well adapted to the Australian grain belt, and commercial cultivars commonly grown by farmers. The research objectives were to: (i) quantify genetic, environmental and GEI effects on T_{crit}; (ii) identify superior wheat genotypes (i.e. with consistently high and stable T_{crit}) across a range of Australian wheat growing conditions; and (iii) identify the major environmental drivers of wheat T_{crit} GEI.

RESULTS

Conditions of growth environments and single-environment analyses

The MET dataset comprised five field and four controlled environments. These were used to assess GEI for wheat PSII heat tolerance (T_{crit}) among the 54 genotypes (Table S1). The METs represented a wide range of growth environments in terms of temperature, relative humidity and photoperiod (Table 1). Across the METs, mean temperature from sowing to anthesis (when T_{crit} was determined) ranged from 9.9 to 17.1°C, and average daily maximum temperature at anthesis ranged from 18.8 to 28.1°C. Mean relative humidity was lowest at Narrabri TOS 2 (37.5%) and highest at Barraport West TOS 1 (73.1%). Photoperiod varied almost twofold between sowing and measurement of T_{crit} at anthesis.

Table 1 Growing period and growth conditions for each environment included in the MET analysis of wheat T_{crit}

Environment[1]	Environment ID	Growing period (sowing to anthesis)[2]	Growing period (sowing to anthesis)[3]			Average 3-day maximum temperature at sampling (°C)
			Mean temperature (°C)	Mean relative humidity (%)	Photoperiod (h)	
Barraport West, VIC TOS 1	VIC-TOS 1	09 May–05 October 2018	9.9	73.5	1574	23.4
Barraport West, VIC TOS 2	VIC-TOS 2	01 June–19 October 2018	10.4	72.0	1228	23.4
Barraport West, VIC TOS 3	VIC-TOS 3	03 July–01 November 2018	11.5	66.9	1382	27.7
Narrabri, NSW TOS 1	NSW-TOS 1	17 May–14 September 2019	13.1	45.6	1279	22.3
Narrabri, NSW TOS 2	NSW-TOS 1	15 July–19 October 2019	14.3	37.5	1104	28.1
Simulated cool season 1	SIM-C1	103 (77) days[4]	12.9	70.8	1007	20.1
Simulated cool season 2	SIM-C2	104 (78) days	12.0	66.7	1019	18.8
Simulated warm season 1	SIM-W1	83 (57) days	17.0	65.3	800	22.8
Simulated warm season 2	SIM-W2	84 (58) days	17.1	67.2	812	23.1

[1]TOS 1, 2 and 3 indicates time of sowing 1, 2 and 3, respectively; VIC, Victoria; NSW, New South Wales.
[2]Anthesis refers to when about 50% of plants were between early and late flowering (Zadoks growth scale between 59 and 70; Zadoks et al., 1974).
[3]Mean environmental conditions for the simulated environments do not include the period prior to when plants were transferred to the growth capsules for the desired simulated growth conditions.
[4]Values in parenthesis indicate the actual period plants were treated to the simulated growing conditions.

Table 2 Estimates of wheat T_{crit} means for each environment and estimates of their genetic and residual variances, and broad-sense heritability from the diagonal genetic variance model of the MET analysis

Environment[1]	Environment ID	*n* genotypes	Mean (± SE)(°C)	Range(°C)	Genetic variance (σ_g^2)	Residual variance (σ_e^2)	Heritability
Barraport West, VIC TOS 1	VIC-TOS 1	20	45.0 ± 0.3	41.8–47.4	0.32	1.24	0.18
Barraport West, VIC TOS 2	VIC-TOS 2	20	46.3 ± 0.2	43.9–48.6	0.22	0.57	0.22
Barraport West VIC TOS 3	VIC-TOS 3	20	46.4 ± 0.2	43.8–49.2	0.54	1.08	0.24
Narrabri, NSW TOS 1	NSW-TOS 1	24	45.7 ± 0.3	41.9–48.4	0.18	0.81	0.25
Narrabri, NSW TOS 2	NSW-TOS 1	23	46.2 ± 0.3	43.2–48.9	0.11	1.36	0.15
Simulated cool season 1	SIM-C1	50	43.6 ± 0.2	42.2–45.5	0.20	0.12	0.74
Simulated cool season 2	SIM-C2	50	43.1 ± 0.1	40.2–44.9	0.19	0.39	0.43
Simulated warm season 1	SIM-W1	50	43.6 ± 0.2	41.2–45.5	0.17	0.20	0.62
Simulated warm season 2	SIM-W2	50	43.3 ± 0.1	41.0–45.2	0.26	0.15	0.75

The diagonal genetic variance model is a baseline model that assumes independence of genetic effects between environments (analogous to analysing each environment separately).
[1]TOS 1, 2 and 3 indicates time of sowing 1, 2 and 3, respectively; VIC, Victoria; NSW, New South Wales.

The initial MET dataset comprised 12 thermal environments but, for the final MET analysis, the three environments in Dingwall, Victoria were excluded because of a lack of significant genetic effects. When testing the genetic effects for the Dingwall trials, we found that there was insufficient evidence to reject the null hypothesis that there is no difference between genotype means, based on the results from the Wald tests. In our case, this means that these environments will not contribute any useful information to understanding the genetic variability in T_{crit}, or how this variability is influenced by environments (genotype by environment interaction). The models fitted to account for variability in each of the environments included in the final MET analysis can be found in Table S5. The lowest and highest mean T_{crit} were 43.1°C (SIM-C2) and 46.4°C (Barraport West TOS 3), respectively, with variation in T_{crit} across the nine environments ranging from 40.2 to 49.2°C (Table 2). There were genetic variances (ranging from 0.11 to 0.54) and residual variances (ranging from 0.12 to 1.40) between environments. Heritability varied considerably among environments (Table 2), being low in the field trials (H^2 = 0.15–0.25), and moderate to high in the simulated environments (H^2 = 0.43–0.75; Table 2).

MET analysis

A summary of the diagonal variance and FA models fitted for the T_{crit} genetic variance is presented in Table 3. The lowest Akaike Information Criterion (AIC) was observed for the FA_1 model (FA model of order 1) with 76 parameters, which only accounted for 42% of the genetic variance

Table 3 Genetic variance models, total number of variance parameters, AIC, residual log-likelihood (loglik) and percentage variance accounted for (% VAF) of the diagonal variance model and FA models of increasing order fitted to the genetic effects for the wheat T_{crit} MET dataset

Model	*n* parameters	AIC	loglik	% VAF
Diagonal	67	690	−278	
FA_1	76	655	−252	42.2
FA_2	81	656	−247	55.6
FA_3	87	662	−244	64.8
FA_4	90	665	−243	95.0
FA_5	95	677	−242	95.3

The FA models are denoted by FA_n (a FA model of order *n*).
AIC, Akaike Information Criterion; FA, factor analytic.

(% VAF). A marginally higher AIC was observed for the FA_2 with 81 parameters, resulting in 56% VAF. In the absence of a consensus of parsimonious model choice based on the AIC and seeking a higher % VAF, we took a holistic assessment of the magnitude of the GEI and changes in heat-maps of the genetic correlations between environments for T_{crit}. Based on these we chose the FA_2 model as our preferred model from which to generate predictions. The FA_2 was not significantly different from either the FA_1 or FA_5 models based on the log-likelihood ratio test (data not shown); however, the FA_2 model captured a satisfactory level of genetic variance for most environments, with only Barraport West TOS 3 having a % VAF less than 50% (Table 4). The first factor (Λ_1) of the FA_2 model explained 50–86% of the variance for all environments, except Barraport West TOS 3 (0.1%) and SIM-W1 (44.9%). The first factor loadings were all positive and on a relatively similar scale. However, the % VAF by the second factor of the FA_2 model for most environments was low (Λ_2, mostly less than 20%), and primarily contrasted three of the simulated environments and Barraport West TOS 1 with the other five environments (Table 4).

Figure 1 presents a combination of a dendrogram of the dissimilarity matrix and a heat-map of the genetic correlation matrix of T_{crit} for the FA_2 model. This shows low to high genetic correlations between environments, indicating substantial GEI. There was little correlation between the warmest environment in Victoria (Barraport West TOS 3) and the other environments, suggesting high GEI. By contrast, correlations were higher among the other eight environments – with the highest correlation observed between Narrabri TOS 2 and SIM-C1 (Figure 1). The clustering of environments in the dendrogram informed the ordering of environments in the genetic correlation matrix. With Barraport West TOS 3 separate, there were two clusters of environments with dissimilarity measures less than 0.43. Cluster 1 comprised the coolest environment in Victoria (Barraport West TOS 1) and the two warm simulated environments (SIM-W1 and SIM-W2), and cluster 2 comprised the remaining five environments excluding Barraport TOS 3.

Selection of genotypes with consistently high T_{crit} (performance and stability) across environments

Genotypes were ranked based on eBLUPs of overall performance (OP) and root mean square deviation (RMSD) – a measure of their sensitivity to changes in environment. The calculation of OP is based on the first factor, while the calculation of RMSD is based on all factors other than the first (Smith & Cullis, 2018), which for our FA_2 model is the second factor. Genotypes 75, 173 and 2454 were ranked among the top three in terms of OP for T_{crit}, and had OP scores of 0.64, 0.52 and 0.59 respectively (Figure 2; Table S6). By contrast, the bottom-ranked three genotypes were 1517, 1752 and 2062 with OP scores of −0.71, −0.59 and −0.49, respectively. Only two of the seven commercial cultivars had a better than average OP, of which Ventura had the highest OP, ranking eighth overall with an OP of 0.32. In addition, Ventura was the least sensitive to change in environment (i.e. had the most stable T_{crit} across

Table 4 REML estimates of rotated factor loadings (first factor, Λ_1; and second factor, Λ_2) and percentage variance accounted for (% VAF) from the FA_2 model fitted to the wheat T_{crit} genetic effects

		Rotated factor loadings		% VAF		
Environment	Environment ID	Λ_1	Λ_2	Λ_1	Λ_2	Λ_1+ Λ_2
Barraport West TOS 1	VIC-TOS 1	0.463	−0.086	62.9	2.2	65.1
Barraport West TOS 2	VIC-TOS 2	0.367	0.158	50.9	9.5	60.3
Barraport West TOS 3	VIC-TOS 3	0.022	0.159	0.1	4.7	4.8
Narrabri TOS 1	NSW-TOS 1	0.308	0.034	52.4	0.6	53.1
Narrabri TOS 2	NSW-TOS 1	0.214	0.098	82.8	17.2	100.0
Simulated cool season 1	SIM-C1	0.414	0.164	86.4	13.6	100.0
Simulated cool season 2	SIM-C2	0.364	−0.002	70.5	0.0	70.5
Simulated warm season 1	SIM-W1	0.276	−0.306	44.9	55.1	100.0
Simulated warm season 2	SIM-W2	0.394	−0.091	58.6	3.1	61.7

TOS 1, 2 and 3 indicates time of sowing 1, 2 and 3, respectively; VIC, Victoria; NSW, New South Wales.

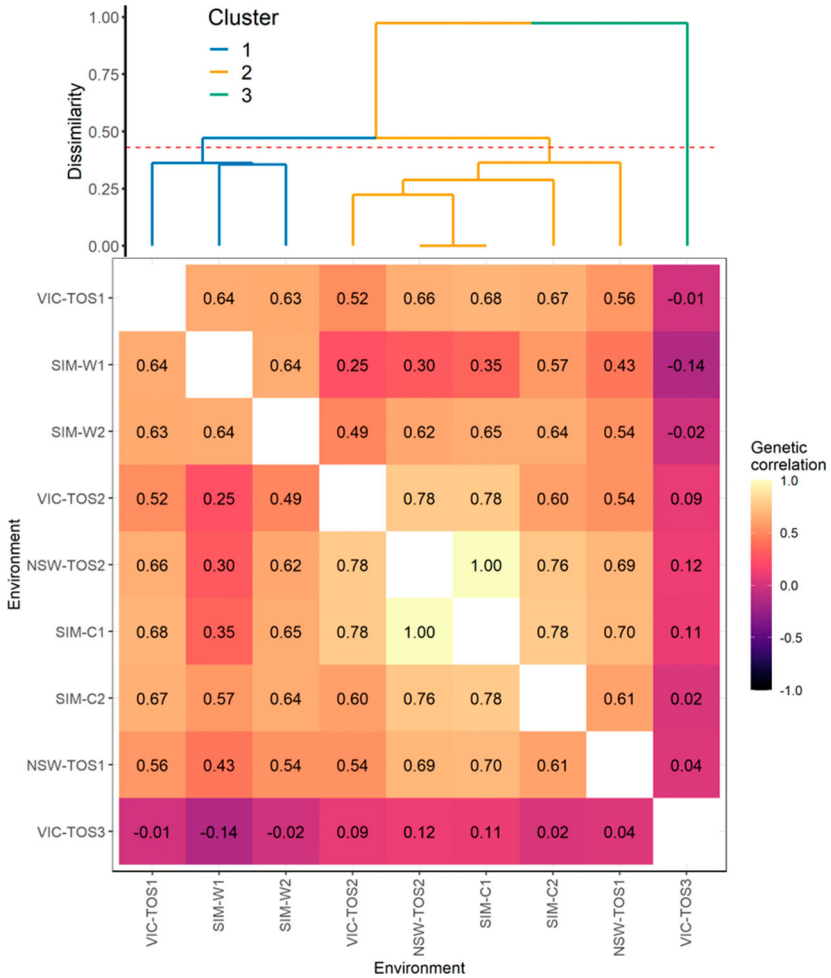

Figure 1. Genetic correlation matrix for wheat T_{crit} for nine environments, ordered by agglomerative hierarchical clustering.
A scale for the genetic correlation is depicted by the colour scale on the right, with a positive and perfect genetic correlation between environments indicated by 1, and a perfect and negative correlation indicated by –1. Estimated correlation coefficients for pairs of environments are indicated within the cells. The nine environments were from field trials in Victoria [Barraport West TOS 1 (VIC TOS 1), Barraport West TOS 2 (VIC-TOS 2) and Barraport West TOS 3 (VIC-TOS 3)] and New South Wales [Narrabri TOS 1 (NSW-TOS 1) and Narrabri TOS 2 (NSW TOS 2)], as well as simulated wheat growing seasons in Canberra [simulated cool season 1 (SIM-C1), simulated cool season 2 (SIM-C2), simulated warm season 1 (SIM-W1) and simulated cool season 2 (SIM-W2)].

environments) with an RMSD of 0.01 (Table S6). Apart from Ventura, Suntop was the only commercial cultivar with a better than average OP, ranking 22nd overall, but it was also the second most sensitive genotype to change in environment (RMSD = 0.275; Figure 2). These results suggest that there are many genotypes with both greater T_{crit} and similar ability to adapt to environmental changes, compared with current commercial cultivars in the germplasm available to Australian wheat breeders.

Correlation of rotated factor loadings with environmental covariates

The main environmental drivers of T_{crit} GEI were identified through correlations of factor loadings with environmental covariates of interest (Table 5). Spearman's rank correlations (ρ) were significant for correlations between the first factor loadings and mean daily temperatures (*cf* ρ = –0.48 to –0.67 with r = –0.50 to –0.82 for 1–30 days before measurement; DBM), and between the second factor loadings and photoperiod (*cf* ρ = 0.59 to 0.68 with r = –0.59 to 0.60 for 1–30 DBM). There were also significant correlations for vapour pressure deficit, solar radiation and photothermal quotient. The Spearman's rank correlations showed strong correlations between mean temperature, relative humidity and vapour pressure deficit assessed between sowing and measurement of T_{crit}, with the first factor loadings (Table 5). The directions of correlations between factor loadings and environmental covariates were mostly the same for temperature, vapour pressure deficit, solar radiation and photoperiod, and opposite to that observed for relative humidity (Table 5). These results indicated that all measured environmental variables potentially influenced T_{crit} GEI, and overall mean growth temperature was the most important. When we focused on temperature as the main driver of T_{crit} GEI and analysed correlations for specific times [i.e. daytime, night time, around noon (0900–1500 h) or 24-h (mean daily)], mean daily temperature was, in most cases, the strongest driver of T_{crit} GEI (Table S7).

DISCUSSION

Wheat breeders aiming to incorporate PSII heat tolerance in their cultivar improvement programmes require critical evaluation of GEI effects on this trait. This is the first report to quantify T_{crit} GEI. Here we show genetic variance and

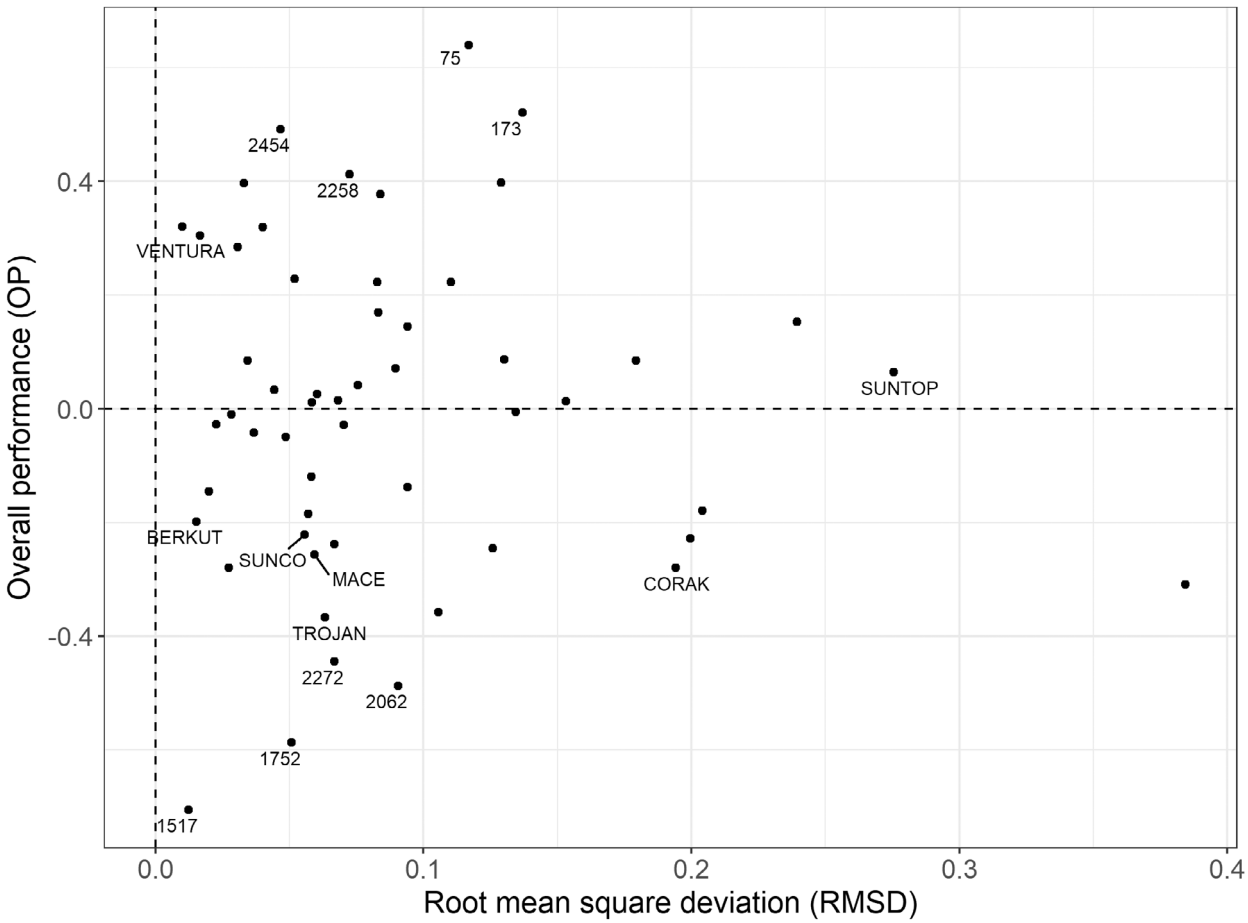

Figure 2. Best linear unbiased predictions of overall performance (OP) versus root mean square deviation (RMSD; a measure of sensitivity of OP across environments) for photosynthetic heat tolerance (T_{crit}) of 54 wheat genotypes, evaluated in nine environments.
Seven commercial cultivars commonly grown by farmers are labelled alongside the highest and lowest ranked four genotypes (according to OP).

Table 5 Spearman's rank correlation coefficients (ρ) for correlations between the rotated factor loadings (first factor, Λ_1; and second factor, Λ_2) of the FA_2 model and environmental covariates for wheat T_{crit}

Growth period	Mean daily						Total daily					
	Temperature		Relative humidity		Vapour pressure deficit		Photoperiod		Solar radiation		Photothermal quotient	
Growth period	Λ_1	Λ_2	Λ_1	Λ_2	Λ_1	Λ_2	Λ_1	Λ_2	Λ_1	Λ_2	Λ_1	Λ_2
1 DBM[1]	−0.67*	0.05	0.43	−0.03	−0.48*	0.08	−0.30	0.68*	**−0.72****	0.38	−0.47	0.57*
3 DBM	−0.34	0.05	0.37	−0.12	**−0.48***	0.23	−0.13	0.60*	−0.42	0.40	−0.29	0.31
7 DBM	**−0.48***	0.13	0.30	−0.50*	−0.43	0.18	−0.27	0.68*	−0.34	0.53	−0.10	0.38
10 DBM	**−0.63***	0.28	0.30	−0.50*	−0.46	0.22	−0.27	0.68*	−0.32	0.57	0.10	0.37
20 DBM	**−0.65***	0.38	0.48*	−0.10	−0.48*	0.25	−0.32	0.60*	−0.30	0.53	0.23	0.39
30 DBM	**−0.67***	−0.05	0.52*	−0.09	−0.48*	0.25	−0.32	0.60*	−0.37	0.55	0.37	0.36
Sowing to measurement	−0.67*	−0.05	**0.77****	0.13	−0.47*	−0.08	−0.02	0.35	−0.40	−0.23	−0.17	0.58*

DBM, days before measurement.
[1]Day before measurement of T_{crit}. * and ** indicates significance at $P \leq 0.05$ and $P \leq 0.01$, respectively. In bold are the highest correlation of environmental variables with the first rotated factor loadings for each defined growth period.

highly variable heritability for wheat T_{crit} (Table 2), as well as significant T_{crit} GEI (Figure 1; Tables 3 and 4). We identified mean daily growth temperature – especially during the 30 days prior to anthesis – as the most likely environmental driver of T_{crit} GEI (Table 5). Interestingly, this period prior to anthesis coincides with rapid spike development (Calderini et al., 2001; Guo et al., 2018), which increases demand for photosynthate. We also identified genotypes consistently superior to commercial cultivars in terms of OP in T_{crit} (Figure 2; Table S6), thus demonstrating inherent potential in the germplasm available to breeders for developing genotypes with greater PSII heat tolerance.

Genetic variance in wheat PSII heat tolerance

Plant breeding for increased stress tolerance and productivity requires the introduction of new and relevant genetic variation, which is easier to source from elite germplasm pre-adapted to the target environment than from exotic sources (Dwivedi et al., 2016). Most genotypes used in this study were an elite subset of heat-tolerant, semi-dwarf germplasm well adapted to the Australian grain belt. The magnitude of genetic variation in wheat T_{crit} in the set of genotypes tested reflected the diversity of germplasm sources and breeding histories. Most genotypes either originated from high-temperature environments or were selected for heat tolerance under high-temperature conditions in Syria, Sudan, Mexico, India and Australia. In these environments, mean growing season and annual maximum temperatures span 16.3–27.7°C and 22.2–36.5°C, respectively. For wheat, a predominantly temperate crop, these environments and temperatures allowed for identification of elite heat-tolerant germplasm. Genetic variation among some of the genotypes used in this study was introduced by targeted crosses between adapted cultivars and heat-tolerant Mexican hexaploid landraces and/or crosses to emmer wheat (*Triticum dicoccon* Schrank) – a heat-tolerant tetraploid – followed by a backcross to the elite adapted cultivar (see Notes in Table S1). Emmer wheat is the progenitor of most cultivated durum wheat, and shows significant variation for heat stress tolerance (Nevo, 2014; Ullah et al., 2018). A recent Australian study (Ullah et al., 2018), examining genetic variability for high-temperature tolerance among hexaploid progenies derived from crosses with emmer wheat, reported that the emmer wheat parents contributed 1–44% of the genome of the derived lines, and that this diversity significantly improved the heat tolerance of the hexaploid materials.

The large genetic variation in wheat T_{crit} reported in this paper indicates significant intraspecies variation that could be exploited in breeding. Similar to ectotherms and non-crop plants, this intraspecies variation in heat tolerance might buffer heat stress via increased thermal safety margins (Araújo et al., 2013; Herrando-Pérez et al., 2019; O'Sullivan et al., 2017; Sunday et al., 2011). Our results show a gradient (i.e. intraspecies variation) in T_{crit} across the 54 wheat genotypes (Figure 2). Some genotypes (e.g. 75, 173 and 2454) could be categorised as high T_{crit}, while others (e.g. genotypes 2062, 1752 and 1517) could be classed as low T_{crit} relative to the commercial cultivars. That some genotypes had a consistently higher and more stable T_{crit} compared with most of the commercial cultivars used in this study indicates potential for significant genetic gains in heat tolerance.

The general understanding of interspecific variation in PSII heat tolerance and links between T_{crit} and environmental temperature is mostly shaped by data from studies of mostly woody, non-crop species (Lancaster & Humphreys, 2020; O'Sullivan et al., 2017; Zhu et al., 2018). One example is the assumption that higher heat tolerance promotes fitness/performance in hotter environments (Araújo et al., 2013). However, Perez and Feeley (2020) indicated that species with higher PSII heat tolerances could be more vulnerable to heat stress due to hotter leaf temperatures and narrower thermal safety margins. In any case, vulnerability is likely related to inhibition of the dark reaction phase of photosynthesis and the export of sugars from leaves, and thus linked to leaf protein content and/or functionality of each of the complexes in the electron transport chain. Molecular mechanisms underpinning genetic variation in wheat T_{crit} may include the induction of heat shock proteins (HSPs), changes in leaf fatty acid composition, and the production of proteins required for assembly and stabilisation of active PSII complexes. Understanding and exploiting these mechanisms is likely to be more relevant to crop improvement than accounting for interspecific variation among other plants, particularly given the large amount of genetic divergence between wheat and the mostly woody species that past photosynthetic heat tolerance research has traditionally examined. Additionally, integrating into models a quantification of GEI effects on T_{crit} could improve projection reliability of climate change impacts on crop production (Pacifici et al., 2015). We also note that our system of determining T_{crit}, although high-throughput, was limited to leaf discs measured hours after detachment and did not allow for whole-plant measurement. Further, the T_{crit} of detached leaves has been observed to reflect conservative estimates of T_{crit} relative to *in situ* levels of PSII heat tolerance (Buchner et al., 2013, 2017).

The experimental field sites for this study were chosen as representative of Australian wheat production practices and environments. Interestingly, we did not detect significant genetic effects on wheat T_{crit} among 20 genotypes in any of the three environments at Dingwall, Victoria, thus these environments were excluded from the MET analysis. It is unclear why genetic effects were not detectable in Dingwall but were present in Barraport West and the other environments among the same set of 20 genotypes. The

Dingwall and Barraport West sites are only 49 km apart; both are in the Mallee district of south-eastern Australia and have a similar climate and relatively infertile soils (Isbell, 2002). Differences in genotype responses across sites suggest a strong environmental and/or management influence on wheat T_{crit}, possibly due to physiological adjustments to microhabitat and leaf temperature changes in response to rainfall and irrigation (timing, amount and form of application; Curtis et al., 2019; Perez & Feeley, 2020). While the total amount of water supplied at Dingwall was lower than Barraport West, both sites received adequate irrigation, and yield of the Dingwall trial was consistently higher than Barraport West (Coast et al., 2021).

Heritability of wheat PSII heat tolerance was highly variable

Heritability is essential for the selection of superior genotypes and the identification of genomic loci that affect the trait of interest. H^2 ranges from 0 (no heritability) to 1 (high heritability). High H^2 indicates that most of the observed phenotypic variation can be attributed to genetics, and therefore response to selection will be high. We observed highly variable broad-sense heritability for wheat T_{crit} – ranging from 0.15 to 0.75 – with clear differences between the field (low H^2) and the controlled environments (medium to high H^2; Table 2). The differences in H^2 between environments reflect the larger residual variances in the field environments compared with the controlled environments. Variability in light levels may have contributed to these differences, with light levels in the growth chambers (although not high at 500–600 μmol m^{-2} sec^{-1}) more stable than in the field. Heritability of wheat PSII heat tolerance was comparable to H^2 reported for leaf cellular membrane stability a different measure of leaf heat tolerance – where values ranged from 0.09 to 0.74 in a variety of crops, including soyabean (*Glycine max* L.; H^2 = 0.09–0.65; Martineau et al., 1979), maize (*Zea mays* L.; H^2 = 0.58; Ottaviano et al., 1991) and spring wheat (H^2 = 0.74; Blum et al., 2001). The range of T_{crit} H^2 in our study is larger than the H^2 previously reported for wheat flag leaf photosynthesis in Australia (0.45–0.65; Silva-Pérez et al., 2020), Mexico (0.33–0.50; Molero & Reynolds, 2020) and the UK (0.50–0.59; Carmo-Silva et al., 2017; Driever et al., 2014). The fact that the range in H^2 for T_{crit} is larger than in other related traits may be partly due to our use of the sound experimental practice of multi-phase experimental design. This sound design, together with advanced statistical analysis techniques, improved the accuracy of genotype comparison by accounting for extraneous sources of trend in both the field and laboratory phases. Success in breeding for heat tolerance has been constrained by the complexity of heat tolerance inheritance, access to appropriate and consistent selection environments (Porch & Hall, 2013), and the resource-intensive and time-consuming nature of such efforts (Driedonks et al., 2016; Kotak et al., 2007). However, recent advances in high-throughput phenotyping, incorporation of more physiological characterisation into molecular marker or genomic selection strategies, followed by extensive evaluation in MET under stress is yielding positive results (Fischer, 2022; Trethowan, 2022).

The high T_{crit} H^2 observed in some of our environments suggest that sustainable genetic gains could be achieved by including T_{crit} as a selection criterion in wheat breeding, a prospect made possible by the development of high-throughput phenotyping tools for T_{crit} (including the one used in this study or reported in Arnold et al., 2021). Indirect selection for higher grain yield through secondary traits with higher heritability and strong associations with grain yield can be more effective than direct selection for grain yield under stress (Bänziger & Lafitte, 1997). However, the association between T_{crit} and grain yield has not been established. Whilst many recent reports assume links between PSII heat tolerance and increased plant fitness under heat stress (Ferguson et al., 2020; Leon-Garcia & Lasso, 2019; Perez & Feeley, 2020; Zhu et al., 2018), there remains a need to validate this relationship more thoroughly. Such studies could ascertain whether or not maintaining a higher T_{crit} translates to better grain yield and quality under heat stress, as well as identifying any associated yield or quality penalties in non-stressed environments. Given the compelling evidence that reproductive organs (including floral organs and developing seeds) are more vulnerable than leaves to heat and drought stresses (Ruan, 2014), and that this susceptibility can be due to poor sink capacity, independent of photosynthesis, as shown in tomato (Li et al., 2012) and maize (Shen et al., 2022), it would also be worth examining the link between leaf T_{crit} and reproductive organ heat tolerance.

MET analysis using FA models showed significant GEI effects on T_{crit}

If genetic gains in heat tolerance are to be achieved by incorporating PSII heat tolerance traits in breeding programmes, a critical assessment of PSII heat tolerance GEI is required. The FA model provided an efficient and realistic way to model the complexity of both the genetic variances and the genetic correlations for wheat T_{crit} GEI effects (Smith et al., 2001, 2015; Smith & Cullis, 2018). Additionally, the flexibility of the linear mixed model in dealing with unbalanced data enabled analysis of the MET data with varying numbers of genotypes (20–50) and replications (2–4) across experiments. Our final FA model accounted for > 50% of the genetic variance in most environments, and up to 100% in three of the nine environments (Table 4). The total variance accounted for across all environments was relatively low and constrained by the poor fit for T_{crit} in Barraport West TOS 3.

The FA models have also been used to define mega-environments in plant breeding programmes (Smith et al., 2015; Smith & Cullis, 2018). Based on the genetic correlations from our final FA model, all environments (excluding Barraport West TOS 3) clustered into two groups (or mega-environments), suggesting strong GEI between these two groups, and weaker GEI within each group. Barraport West TOS 3 shared particularly low genetic correlations with the other eight environments (Figure 1). By contrast, the high genetic correlations between environments within clusters 1 and 2 suggests there were similar genetic responses for environments within a cluster (i.e. low GEI). Narrabri TOS 2 was closely correlated with the two simulated cool seasons, especially SIM-W1 (Figure 1). From a phenotyping perspective, these strong correlations indicate that the APPF Growth Capsules can be used in conjunction with field experiments to evaluate wheat T_{crit}.

Our study provides a sound foundation for further investigating the extent to which photosynthetic heat tolerance can improve grain yield, and supports the targeting of PSII heat tolerance in Australian wheat breeding. However, it remains a single study of a single trait, and thus its contribution to overall wheat heat tolerance improvement is limited given that many other traits also contribute to heat tolerance. For greater impact, T_{crit} GEI should be considered alongside other relevant energy metabolism-related physiological traits. For example, our recent works showed that elevated temperature elicited a stronger response from wheat mitochondrial dark respiration (measured as O_2 consumption rate, $R_{dark\_}O_2$) than from photosynthesis, as well as a greater $R_{dark\_}O_2$ response to night warming rather than day warming (Coast et al., 2021; Posch et al., 2021). Warm nights also led to declines in biomass and leaf and root $R_{dark\_}O_2$ and increased alternative oxidase pathway capacity, suggesting a reduction in plant energy demand under warm nights. The strong links between biomass decline, photosynthesis and respiration under heat stress strengthen the case for a multi-faceted approach to cultivar improvement that exploits a combination of respiratory heat tolerance traits (e.g. T_{max} of R_{dark}, the temperature at which R_{dark} peaks prior to respiratory function rapidly declining) and T_{crit}.

Wheat T_{crit} at anthesis is strongly influenced by mean daily growth temperature preceding anthesis

Our results show that T_{crit} of PSII in wheat flag leaves was influenced by all measured environmental covariates. However, mean daily temperature correlated best or second best with first factor loadings for all periods, except 3 days prior to anthesis. Growth temperature is one of the most influential environmental drivers of photosynthesis (Atkin & Tjoelker, 2003; Hikosaka et al., 2005; Wright et al., 2006), and within the photosynthetic machinery the thylakoid membrane-embedded PSII is particularly heat sensitive (Armond et al., 1978). That mean daily temperature was correlated with T_{crit} in the short (1 day prior to anthesis), medium (7–30 days prior to anthesis) and long (sowing to anthesis) terms likely reflects different scales of mechanistic adjustments in the leaf. Adjustments due to temperature stress in the short term may be underpinned by biochemical changes, such as increased relative abundance of saturated fatty acids (Zhu et al., 2018), expression of HSPs (Vierling, 1991) and/or changes in the concentration of key metabolites (Kaplan et al., 2004). On the other hand, medium- and/or long-term associations presumably relate to changes of thylakoid membranal and leaf functional traits that require greater investment in PSII. Such investments in membranal characteristics may be related to repairs of PSII, for example, curvature, thickness and stromal gaps (Theis & Schroda, 2016; Yoshioka-Nishimura, 2016), as well as leaf structural and morphological traits (e.g. higher leaf mass per area, leaf thickness and density) that confer high-temperature tolerance (e.g. species with higher leaf mass per area have higher photosynthetic heat tolerance; Sastry & Barua, 2017; Wright et al., 2005).

In addition to links between T_{crit} and environmental covariates that span various days prior to measurement of T_{crit}, we specifically investigated links between T_{crit} and growth temperatures of specific time frames (i.e. daytime, night-time, midday and a 24-h period). T_{crit} was mostly dependent upon mean daily temperature. We had expected a stronger link between T_{crit} and the higher temperatures around midday. However, in the Australian context, the strong relationship between mean daily temperature and T_{crit} was still notable given that wheat yield losses have been attributed to a combination of increasing mean daily temperatures and heatwaves (Ababaei & Chenu, 2020).

CONCLUSION

Genetic variance for T_{crit} in a subset of Australian wheat breeding germplasm demonstrates potential for significant genetic gains in heat tolerance. Our results revealed significant T_{crit} GEI, as well as identified mean daily growth temperature prior to anthesis as the major environmental driver of T_{crit} GEI – both supporting the potential development of high-temperature-tolerant wheat. The potential gains of incorporating T_{crit} in breeding programmes are worth exploring despite heritability for T_{crit} in the field being relatively low. Links between wheat T_{crit} and crop performance should be investigated further to ascertain whether or not higher T_{crit} translates to improved grain yield and quality under heat stress, as well as whether high T_{crit} bears any yield or quality penalties in non-stressed environments.

EXPERIMENTAL PROCEDURES

A total of 54 wheat genotypes (Table S1) were grown in eight field and four controlled environments over 3 years (2017–2019). Of

these 54 genotypes, 20 were common to all environments. The eight field experiments were conducted in major wheat-growing regions of Australia (Dingwall, Victoria in 2017, Barraport West, Victoria in 2018, and Narrabri, New South Wales in 2019). The field trials were sown 1 month apart over 3 months in 2017 and 2018, and 2 months apart in 2019, with the initial sowing time being the optimum sowing time for each region. Later sowing exposed plants to higher temperatures at the critical reproductive and grain-filling stages of development. Across the different trials, plants received water from a combination of rainfall and irrigation of 152–185 mm in Dingwall, 217–235 mm in Barraport West, and 363–492 mm in Narrabri between sowing and anthesis. Twenty genotypes were evaluated during the 2017 and 2018 trials, and 24 genotypes in 2019. The experimental designs, crop husbandry and data collection methods were similar across all three field experiments, except for the differences mentioned above (i.e. number of sowings and genotypes). A detailed description of the 2017 and 2018 experimental sites, designs and crop husbandry are reported in Coast et al. (2021), while those for the 2019 experiments are given below.

2019 field trial with 24 genotypes

Experimental site. The 2019 field experiment was conducted at the Plant Breeding Institute (PBI; 30.27°S, 149.81°E; elevation 212 m above sea level) of The University of Sydney, Narrabri, NSW. Narrabri is characterised by hot summers and mild winters with a summer-dominant rainfall pattern. Long-term mean daily maximum and minimum temperatures during the wheat growing season at Narrabri range from 7.1–21.3°C in May (optimal sowing time) to 11.4–26.94°C in October (during anthesis) and 16.9–32.1°C in December (at harvest). Mean rainfall from sowing (in May) to anthesis (in October) at Narrabri is 273 mm. Temperature, relative humidity, rainfall and windspeed data were recorded onsite with a weather station. The soil in Narrabri is a cracking, montmorillonitic clay soil characterised as a grey vertosol (Isbell, 2002).

Experimental design. The 2019 field experiment used a two-phase experimental design following the definition of Brien and Bailey (2006) to investigate the response of T_{crit} of 24 genotypes to warmer growth conditions. This was employed to account for variation due to the experimental layout in the field (field phase) and on the 48-well plate used in the laboratory for determining T_{crit} (laboratory phase). The two-phase experimental design was implemented to separate potential sources of variation into components, thus improving the estimate of treatment effects (Cullis et al., 2003; Curnow, 1959).

The field phase focused on 24 wheat genotypes that formed part of a larger set of 30 wheat genotypes in a time of sowing (TOS) trial. The experiment was arranged in two trials (or main blocks) subdivided into four replicate blocks. The two main blocks represented recommended sowing (Narrabri TOS 1) and late-sown (Narrabri TOS 2) environments, and were treated as two trials each containing four replicate blocks. Each replicate block consisted of 30 plots arranged in five rows and six columns. Wheat genotypes were randomly allocated to the plots within each replicate block following a randomised complete block design. Narrabri TOS 1 was sown on 17 May 2019 and Narrabri TOS 2 was sown on 15 July 2019. Flag leaf tissue was taken from one randomly selected plant in each field plot (see Flag leaf sampling section below). A total of 192 leaf tissue samples from 24 genotypes, four blocks and two TOS were collected. These samples formed the experimental units for the laboratory phase of the experiment.

The laboratory phase of the experiment was based on an Incomplete Block Design across 12 blocks with 24 units per block, with the initial starting array generated from the CycDesigN package (VSN-International, Hemel Hempstead, UK). The laboratory phase was conducted separately for each TOS, as partially replicated designs (Cullis et al., 2006) with 1.5 replicates of 96 treatments, where the 96 treatments comprised a factorial treatment structure of four field replicates by 24 genotypes. Laboratory analysis was conducted over 6 days: three consecutive days each for Narrabri TOS 1 and Narrabri TOS 2. Each day comprised two incomplete blocks. The starting Incomplete Block Design was optimised for the layout of samples across the 48-well plate using the optimal design (od) package in R (Butler, 2013). The leaf samples were positioned across a 6 × 8 spatial array, based on the dimensions of the Peltier block described in the next section.

2019 controlled environment trial with 50 genotypes

In addition to the field trials, a trial with 50 wheat genotypes (including 20 genotypes common to the field trials) was conducted in four high-precision Growth Capsules, with independent control of temperature, relative humidity and multispectral LED light. The Growth Capsules were managed by the Australian Plant Phenomics Facility (APPF) and Grain Phenomics Climate Facility at the Australian National University (ANU), Canberra (https://www.plantphenomics.org.au). Each Growth Capsule comprised two separate chambers 3.8 m wide × 1.1 m deep × 2.1 m high. These Growth Capsules are capable of simulating location-specific environmental conditions, including diurnal and seasonal changes and complex climate scenarios, thus enabling phenotypic comparison and screening of large numbers of genotypes across various environments. The chambers were used to dynamically simulate four environments: two cool and two warm (approximately 5°C higher than the cool) wheat-growing seasons, based on the 15-min average temperature from the vegetative growth period to the end of anthesis (June–October) each year from 2013 to 2018 for the Narrabri site. Simulation of dawn, daylight and dusk timings also mimicked conditions in Narrabri. Lights were supplied by colour-adjustable LED modules that were kept thermally insulated from the plant growth area. The simulated environments will henceforth be identified as simulated cool season 1 (SIM-C1), simulated cool season 2 (SIM-C2), simulated warm season 1 (SIM-W1) and simulated warm season 2 (SIM-W2).

Crop husbandry. Germinated seeds of the 50 wheat genotypes were sown into 6-L plastic pots (one seedling per pot) filled with Martins potting mix (Martins Fertilizers, Yass, NSW Australia). Martins potting mix is a formulation of organic composted materials, coir, water storage crystals, controlled-release fertiliser, trace elements and wetting agent. The Martins mix was supplemented with 4 g L^{-1} of Osmocote® OSEX34 EXACT slow-release fertiliser (Scotts Australia, Bella Vista, NSW, Australia) and treated at 63°C for 1 h prior to filling pots. Plants were grown for 3 weeks under glasshouse conditions at the ANU Controlled Environment Facilities, Canberra, Australia. In the glasshouse, plants were exposed to natural light with average daylength of 11.8 h, and daily light integral of 14.9 mol m^{-2} d^{-1}. Daily temperature and relative humidity were on average 19.4°C and 54.8%, respectively. Thereafter plants were transferred to the high-precision Growth Capsules described earlier, where they were initially kept for 1 week at constant day:night temperatures of 20:15°C, with photosynthetically active radiation at plant height of 500–600 μmol m^{-2} sec^{-1} on a 12-h photothermal regime. Following this week, the environmental conditions within the chambers were programmed to either a cool

(SIM-C1 and SIM-C2) or warm (SIM-W1 and SIM-W2) thermal regime. For SIM-C1 and SIM-C2, which were based on Narrabri 2013–2018 June–October weather, average daily maximum temperature varied from 16.8 to 39.3°C, and average daily minimum temperature varied from −4.3 to 12.2°C. For SIM-W1 and SIM-W2, the chambers were set to 5°C higher than SIM-C1 and SIM-C2. General plant management followed the established protocol of the APPF and Grain Phenomics Climate Facility at ANU with additional control for powdery mildew and aphids as required.

Experimental design. Plants were randomly positioned on benchtops in the chambers, following a randomised complete block design with two replicates per genotype. This resulted in a total of 200 plots in phase one of the experiment. Because the laboratory phase of estimating T_{crit} was limited to 48 samples per run, a laboratory phase design was created with 6 blocks of 24 units per block, totalling 144 leaf samples. Thus, the laboratory design followed a partially replicated design and was unbalanced with three leaf samples for most genotypes (one sample from chamber replicate one and two samples from chamber replicate two or vice-versa). However, four genotypes were limited to one single leaf sample from each environmental replicate. Due to differences in genotype maturity in the cool and warm environments, samples were collected separately. All samplings were done when plants were at the same developmental stage – at anthesis (Zadoks growth stage 60–69; Zadoks et al., 1974). Genotypes grown in the warm environments were collected prior to those in the cool environments, each being sampled over three consecutive days at 48 samples per day. Like the 2019 field experiment, the design of the controlled environment study, with the initial starting array, was generated using the CycDesigN package (VSN-International, Hemel Hempstead, UK), and the starting design was optimised for the layout of samples across the 48-well plate using the optimal design (od) package in R (Butler, 2013).

Flag leaf sampling and determination of T_{crit}

Flag leaves were harvested when at least 50% of the genotypes were at anthesis. In the field, leaves were harvested from plants from one of the inner three rows of five-row plots between 08:30 and 10:30 hours. In the chambers, flag leaves of main tillers at anthesis were harvested between 08:45 and 11:00 h. Immediately after harvesting a flag leaf, a section of approximately 3–4 cm was cut from the middle. The middle and upper sections of the leaves were kept in resealable bags and dark-adapted for between 1.5 and 6 h prior to estimating T_{crit} (middle section). In a previous experiment, we determined that dark-adapting leaves for between 1.5 and 6.5 h post-excision from plant had no significant effect ($P = 0.189$) on T_{crit} (Supplementary Information S1 and Table S2).

Wheat T_{crit} was determined using a custom-built system that combined an imaging fluorometer (FluorCam 800MF, Photon Systems Instrument, Brno, Czech Republic), a thermoregulator attached to the fluorometer (TR2000, Photon Systems Instrument, Brno, Czech Republic) and a 48-well Peltier block. The Peltier block measured 8 × 12 cm, and each well on the block was 1 cm in diameter. This set-up was capable of temperature regulation within the 10–70°C range with accuracy of ± 0.1°C. Single leaf discs (~6 mm diameter) were excised from the middle sections of the detached dark-adapted flag leaves and placed atop 90 μl of tap water in the wells of the Peltier block. Water was supplied to prevent water stress during the assay. In addition, a transparent glass plate covered the wells to reduce evaporative loss during the subsequent application of a heat ramp (i.e. a constant rate of temperature increase). The Peltier block was positioned 14 cm below a charge-coupled device camera within the fluorometer for imaging. Leaf discs were warmed at a constant rate of 1°C min^{-1} from 20 to 65°C, consistent with generally used measurement protocols (Schreiber & Berry, 1977; Weng & Lai, 2005; Zhu et al., 2018). Mean surface temperatures of leaf discs increased at a similar rate to the programmed temperature and block surface temperature, but were generally cooler (by 0.9–3.9°C, Supplementary Information S2; Figure S1). Throughout the temperature ramp the imaging fluorometer measured the minimum chlorophyll fluorescence (F_0) of leaf discs at approximately 1-min intervals. Fluorescence was measured by excitation using short flashes (10 μsec) of extremely weak blue light. The FluoroCam 7.0 software package (Photon Systems Instrument, Brno, Czech Republic) was used to pre-process captured images, and to export the temperature and fluorescence data. Wheat T_{crit} was determined from the temperature and fluorescence data according to the method of Schreiber and Berry (1977), using the package segmented (Muggeo, 2003, 2008, 2016, 2017) in the R statistical environment (R-Core-Team, 2021). The segmented package estimates linear and generalised linear models, and iteratively identifies the breakpoint based on the best fit model. The breakpoint was taken as T_{crit}, along with the estimate of its standard error. Using the segmented package is preferred to deriving T_{crit} traditionally from the intersection point of two regression lines extrapolated from the flat and steep portion of the temperature-dependent F_0 response curve (Knight & Ackerly, 2003; O'Sullivan et al., 2017; Schreiber & Berry, 1977) as it eliminates human bias in selecting the intersection point and provides an estimate of standard error for T_{crit}.

Statistical analysis

Analysis of the T_{crit} data was undertaken in three parts: (1) single environment analysis; (2) MET analysis; and (3) correlations of FA model loadings with environmental variables (Figure S2; Tables S3 and S4). In the first part, linear mixed models for each individual environment were fitted, with fixed, random and residual terms accounting for the treatment effects and design effects relevant to the different experimental layouts in each environment. Genotype was fitted as a fixed effect for these individual environment analyses. Spatial effects were assessed, and the required terms fitted, using the method of Gilmour et al. (1997) and Cullis et al. (2003). The Dingwall and Barraport West trials consisted of only a single phase, so the models for the environments in these trials included design and spatial terms relevant to this single phase. For the Narrabri trial, with a two-phase experimental design spanning both the field and the laboratory, the models for these environments accounted for both the field phase design and spatial effects, and the laboratory phase design and spatial effects. The laboratory phase effects considered included spatial effects on the Peltier block wells, and design effects induced by sampling across days and the incomplete block design (described previously). Due to identical randomisation of the chamber material to the laboratory phase for the four simulated environments, it was impossible to separate the chamber spatial variability from spatial variability across wells. As such, each chamber was assumed to be its own environment, and the analyses of these environments were undertaken as independent single-phase analyses. Diagnostic residual plots were used to check assumptions of normality and homoscedasticity of residuals made during model fitting, and to visualise spatial trends along rows and columns. Log-likelihood ratio tests were used to test changes in the random spatial effects between models, and Wald tests were used to assess the significance of fixed spatial effects, to select the most parsimonious model for each environment. The selected models were examined for significant genetic effects using Wald tests. Environments that

showed significant genetic effects for T_{crit} were then incorporated in the second step of the analysis. However, environments that were found to have no significant genetic effects in the preliminary single site analyses were omitted from the subsequent MET analysis. The null hypothesis for testing a treatment effect is that there is no difference between treatment means. As such, a lack of significant genetic effects in an environment indicates that there are no significant differences in genotype performance within that environment for the trait of interest.

The second part of the analysis combined data from the environments with significant genetic effects into a MET analysis. Initially, a diagonal variance model was fitted to the GEI effects, which allowed for heterogeneous genetic variances for each environment. The diagonal genetic variance model was used as a baseline model that assumed independence of the GEI effects between environments; thus, it was analogous to analysing each environment separately. Broad-sense heritability (H^2) was estimated following the method of Cullis et al. (2006) for each environment using the diagonal genetic variance model. This was estimated as:

$H^2 = 1 - \frac{A_{tt}}{2\gamma_v}$, where A_{tt} is the average pairwise prediction error variance of the genotype effects, and γ_v is the genetic variance, for a particular environment.

Subsequently, FA models (FA_n, with n in this case indicating the order of the FA model from 1 to 5; Smith et al., 2001) were fitted to allow for heterogeneity in both the genetic variances for each environment and the genetic correlations between environments. The diagonal variance model and FA_n models were compared to select a final genetic variance model for the MET analysis. Model comparisons involved a holistic assessment of log-likelihood ratio tests, values of AIC (Bozdogan, 1987), and the percentage of genetic variance accounted for by the factors (Beeck et al., 2010; % VAF; Smith & Cullis, 2018). The final MET model was used to obtain predictions of the GEI effects via empirical best linear unbiased predictions (eBLUPs), as well as genetic variances for each environment, and genetic correlations between each pair of environments. The genetic correlations indicated the presence or absence of GEI, with high positive correlations between environments corresponding to low GEI (i.e. genotypes have similar T_{crit} rankings across multiple environments). To identify superior genotypes across environments (i.e. those with consistently high and stable T_{crit}), measures of OP and stability/sensitivity (defined as RMSD) from the FA selection tools (FAST) method proposed by Smith and Cullis (2018) were used. Lower RMSD values for genotypes indicate lower sensitivity of those genotypes to environmental conditions in terms of T_{crit}.

The third part of the analysis focussed on correlations of FA model loadings with environmental variables. Correlation coefficients between rotated factor loadings from the final FA models and environmental covariates for specified periods preceding anthesis were estimated using Spearman's rank correlations. The environmental covariates were growth air temperature, relative humidity, vapour pressure deficit, photoperiod and solar radiation. Photothermal quotient – the ratio of mean daily incident or intercepted radiation to mean temperature – was also correlated with the rotated factor loadings. Photothermal quotient for the controlled environments was computed using daily light quantity in the chambers – the quantity of photons in the photosynthetic range integrated over the day (daily light integral). These correlation coefficients were used to identify the most likely environmental drivers of T_{crit} GEI.

Analyses were conducted using the ASReml-R software (Butler et al., 2017) within the R statistical environment (R-Core-Team, 2021) and Genstat (21st ed. VSN International, Hemel Hempstead, UK). ASReml-R estimates variance parameters of linear mixed models using Residual Maximum Likelihood (REML; Patterson & Thompson, 1971). In addition to ASReml, the R packages, 'ASExtras4' (Butler, 2015), 'myf' (Butler, 2014) and 'reshape2' (Wickham, 2007) were required for analysis, and 'ggrepel' (Slowikowski, 2021), 'cluster' (Maechler et al., 2021) and 'ggplot2' (Wickham, 2016) for visualisation of results.

ACKNOWLEDGEMENTS

The authors acknowledge and celebrate the First Australians on whose traditional lands this research was undertaken, and pay our respect to the elders past and present. This work was supported by grants from the ARC Centre of Excellence in Plant Energy Biology (CE140100008), and the Australian Grains Research and Development Corporation (GRDC) Postdoctoral Fellowship: Photosynthetic Acclimation to High Temperature in Wheat (US1904-003RTX – 9177346), National Wheat Heat Tolerance Project (US00080), and Statistics for the Australian Grains Industry (SAGI) – Northern Node Project (DAQ1606-003RTX). Onoriode Coast received support from Research England's 'Expanding Excellence in England' (E3)-funded Food and Nutrition Security Initiative of the Natural Resources Institute, University of Greenwich. Bradley C. Posch was supported by the Australian Government Research Training Program. The authors are grateful to the Australian Plant Phenomics Facility (APPF) for use of their growth capsules. The APPF is supported under the National Collaborative Research Infrastructure Strategy of the Australian Government. The authors thank Dr Richard Poire-Lassus for managing the growth capsules. The authors also thank Amy Smith of Birchip Cropping Group, Victoria, for help with field trials in Victoria, and Sabina Yasmin for managing the trial at Narrabri. The authors are grateful to the farmers who generously provided us with field sites for the 2017 and 2018 trials. Staff of the ANU Research School of Biology Plant Services team, especially Christine Larsen, Jenny Rath, Gavin Pritchard and Steven Dempsey, are thanked for maintaining the plants in the controlled environments. Open access publishing facilitated by Australian National University, as part of the Wiley - Australian National University agreement via the Council of Australian University Librarians.

AUTHOR CONTRIBUTIONS

OC, HB, ML, Y-LR and OKA acquired the funding. OC, BCP, HB, CP, AMK, ML, Y-LR and OKA conceptualised and designed the experiments. RT provided the wheat germplasm. OC, BCP, CP, HB and OKA managed the project. OC, BCP, OG and JM performed the experiments. OC, BCP and BGR analysed the data with help from AMK. All authors contributed to the interpretation of results. OC and BGR wrote the initial drafts with support and further inputs from BCP, HB, AMK, RT and OKA. All authors finalised the manuscript draft. All authors read and approved the final version for publication.

CONFLICT OF INTEREST

The authors declare that there are no conflicts of interest.

DATA AVAILABILITY STATEMENT

Raw T_{crit} for all genotypes and environmental data for all experiments are provided as supplementary information files in Workbooks S1 and S2. Custom R scripts may be requested from the corresponding authors.

SUPPORTING INFORMATION

Additional Supporting Information may be found in the online version of this article.

Table S1. Pedigree information for 54 wheat genotypes used in this study

Table S2. Effect of time from harvest and dark adaptation on flag leaf T_{crit} of wheat cultivars Trojan and Suntop

Table S3. Information about experimental designs for experiments conducted as part of the MET investigation of wheat T_{crit}

Table S4. Environmental variables correlated with rotated factor loadings of the FA_2 model for specified growth periods preceding anthesis. The growth periods were 1, 3, 7, 10, 20 and 30 DBM of T_{crit}, and from sowing to measurement of T_{crit}

Table S5. Fixed, random and residual model terms fitted for each environment and used in the final MET analysis

Table S6. Ranking of wheat genotypes based on OP of T_{crit} from the MET analysis

The RMSD values are included as a measure of sensitivity of genotypic performance to environmental conditions. Lower RMSD values indicate lower sensitivity. Data are presented for the seven commercial cultivars, used as checks, and the highest and lowest four ranked genotypes based on OP.

Table S7. Spearman's rank correlation coefficients (ρ) for correlations between the rotated factor loadings (first factor, Λ_1; and second factor, Λ_2) of the FA_2 model (a FA model of order 2) and growth environment temperature over 24 h (all day), from sunrise to sunset, at about midday (0900–1500 h), and at night (sunset to sunrise) for wheat T_{crit}

Figure S1. Plots of relationship between the temperatures on the Peltier heating block against temperatures of water in the heating block wells (blue circles), and of leaf discs placed directly on the surface of the water plate (orange circles). The Peltier heating blocks were set to ramp the temperature from 20 to 60°C at a constant rate of rate of 1°C min^{-1}. Linear regression for water was $y = -0.93x + 1.40$ (R^2=0.99) and for leaf discs was $y = 0.96x - 0.88$ ($R^2 = 0.99$).

Figure S2. Flow chart of data analysis.

Data S1. T_{crit} MET Dataset

Data S2. Environmental covariates

REFERENCES

Ababaei, B. & Chenu, K. (2020) Heat shocks increasingly impede grain filling but have little effect on grain setting across the Australian wheatbelt. *Agricultural and Forest Meteorology*, **284**, 107889.

ABARES Agricultural Commodity Statistics (2021) Australian Bureau of Agricultural and Resource Economics and Sciences, Canberra, Australia. Available at: https://www.agriculture.gov.au/abares/research-topics/agricultural-outlook/data#2020 [Accessed on 21 August 2021]

Araújo, M.B., Ferri-Yáñez, F., Bozinovic, F., Marquet, P.A., Valladares, F. & Chown, S.L. (2013) Heat freezes niche evolution. *Ecology Letters*, **16**, 1206–1219.

Armond, P.A., Schreiber, U. & Björkman, O. (1978) Photosynthetic acclimation to temperature in the desert shrub, *Larrea divaricata*: II. Light-harvesting efficiency and electron transport. *Plant Physiology*, **61**, 411–415.

Arnold, P.A., Briceño, V.F., Gowland, K.M., Catling, A.A., Bravo, L.A. & Nicotra, A.B. (2021) A high-throughput method for measuring critical thermal limits of leaves by chlorophyll imaging fluorescence. *Functional Plant Biology*, **48**, 634–646.

Asseng, S., Cammarano, D., Basso, B., Chung, U., Alderman, P.D., Sonder, K. *et al.* (2017) Hot spots of wheat yield decline with rising temperatures. *Global Change Biology*, **23**, 2464–2472.

Asseng, S., Ewert, F., Martre, P., Rötter, R.P., Lobell, D.B., Cammarano, D. *et al.* (2015) Rising temperatures reduce global wheat production. *Nature Climate Change*, **5**, 143–147.

Atkin, O.K. & Tjoelker, M.G. (2003) Thermal acclimation and the dynamic response of plant respiration to temperature. *Trends in Plant Science*, **8**, 343–351.

Azam, F.I., Chang, X. & Jing, R. (2015) Mapping QTL for chlorophyll fluorescence kinetics parameters at seedling stage as indicators of heat tolerance in wheat. *Euphytica*, **202**, 245–258.

Bänziger, M. & Lafitte, H. (1997) Efficiency of secondary traits for improving maize for low-nitrogen target environments. *Crop Science*, **37**, 1110–1117.

Beeck, C.P., Cowling, W.A., Smith, A.B. & Cullis, B.R. (2010) Analysis of yield and oil from a series of canola breeding trials. Part I. Fitting factor analytic mixed models with pedigree information. *Genome*, **53**, 992–1001.

Berry, J. & Bjorkman, O. (1980) Photosynthetic response and adaptation to temperature in higher-plants. *Annual Review of Plant Physiology and Plant Molecular Biology*, **31**, 491–543.

Blum, A., Klueva, N. & Nguyen, H.T. (2001) Wheat cellular thermotolerance is related to yield under heat stress. *Euphytica*, **117**, 117–123.

Bozdogan, H. (1987) Model selection and Akaike's Information Criterion (AIC): the general theory and its analytical extensions. *Psychometrika*, **52**, 345–370.

Brien, C.J. & Bailey, R.A. (2006) Multiple randomizations. *Journal of the Royal Statistical Society: Series B (Statistical Methodology)*, **68**, 571–609.

Buchner, O., Karadar, M., Bauer, I. & Nuener, G. (2013) A novel system for *in situ* determination of heat tolerance of plants: first results on alpine dwarf shrubs. *Plant Methods*, **9**, 7.

Buchner, O., Roach, T., Gertzen, J., Schenk, S., Karadar, M., Stöggl, W. *et al.* (2017) Drought affects the heat-hardening capacity of alpine plants as indicated by changes in xanthophyll cycle pigments, singlet oxygen scavenging, α-tocopherol and plant hormones. *Environmental and Experimental Botany*, **133**, 159–175.

Butler, D. (2014). myf: Utility functions for asreml objects. R package version 1.0.

Butler, D. (2015). ASExtras4: utility functions for asreml objects. R package version 1.0.

Butler, D.G. (2013) *On the Optimal Design of Experiments under the Linear Mixed Model*. Australia: The University of Queensland.

Butler, D.G., Cullis, B.R., Gilmour, A.R., Gogel, B.G. & Thompson, R. (2017) *ASReml-R Reference Manual Version 4*. Hemel Hempstead, United Kingdom: VSN International Ltd.

Calderini, D.F., Savin, R., Abeledo, L.G., Reynolds, M.P. & Slafer, G.A. (2001) The importance of the period immediately preceding anthesis for grain weight determination in wheat. *Euphytica*, **119**, 199–204.

Carmo-Silva, E., Andralojc, P., Scales, J., Driever, S., Mead, A., Lawson, T. *et al.* (2017) Phenotyping of field-grown wheat in the UK highlights contribution of light response of photosynthesis and flag leaf longevity to grain yield. *Journal of Experimental Botany*, **68**, 3473–3486.

Coast, O., Posch, B.C., Bramley, H., Gaju, O., Richards, R.A., Lu, M. *et al.* (2021) Acclimation of leaf photosynthesis and respiration to warming in field-grown wheat. *Plant, Cell & Environment*, **44**, 2331–2346.

Comstock, R. (1977) Quantitative genetics and the design of breeding programs. In: Pollak, E., Kempthorne, O. & Bailey, T.B. Jr. (Eds.) *Proceedings of the International Conference on Quantitative Genetics*. Ames, USA: Iowa State University Press, pp. 1705–1718.

Cullis, B.R., Smith, A.B. & Coombes, N.E. (2006) On the design of early generation variety trials with correlated data. *Journal of Agricultural, Biological, and Environmental Statistics*, **11**, 381–393.

Cullis, B.R., Smith, A.B., Panozzo, J.F. & Lim, P. (2003) Barley malting quality: are we selecting the best? *Australian Journal of Agricultural Research*, **54**, 1261–1275.

Curnow, R. (1959) The analysis of a two phase experiment. *Biometrics*, **15**, 60–73.

Curtis, E.M., Knight, C.A. & Leigh, A. (2019) Intracanopy adjustment of leaf-level thermal tolerance is associated with microclimatic variation across the canopy of a desert tree (*Acacia papyrocarpa*). *Oecologia*, **189**, 37–46.

Dreccer, M.F., Condon, A.G., Macdonald, B., Rebetzke, G.J., Awasi, M.-A., Borgognone, M.G. *et al.* (2020) Genotypic variation for lodging tolerance in spring wheat: wider and deeper root plates, a feature of low lodging, high yielding germplasm. *Field Crops Research*, **258**, 107942.

Driedonks, N., Rieu, I. & Vriezen, W.H. (2016) Breeding for plant heat tolerance at vegetative and reproductive stages. *Plant Reproduction*, **29**, 67–79.

Driever, S., Lawson, T., Andralojc, P., Raines, C. & Parry, M. (2014) Natural variation in photosynthetic capacity, growth, and yield in 64 field-grown wheat genotypes. *Journal of Experimental Botany*, **65**, 4959–4973.

Dwivedi, S., Ceccarelli, S., Blair, M., Upadhyaya, H., Are, A. & Ortiz, R. (2016) Landrace germplasm for improving yield and abiotic stress adaptation. *Trends in Plant Science*, **21**, 31–42.

Ferguson, J.N., McAusland, L., Smith, K.E., Price, A.H., Wilson, Z.A. & Murchie, E.H. (2020) Rapid temperature responses of photosystem II efficiency forecast genotypic variation in rice vegetative heat tolerance. *The Plant Journal*, **104**, 839–855.

Fischer, R.A. (2022) History of wheat breeding: a personal view. In: Reynolds, M.P. & Braun, H.-J. (Eds.) *Wheat Improvement: Food Security in a Changing Climate*. Springer Nature: Switzerland, pp. 17–30.

Geange, S.R., Arnold, P.A., Catling, A.A., Coast, O., Cook, A.M., Gowland, K.M. *et al.* (2020) The thermal tolerance of photosynthetic tissues: a global systematic review and agenda for future research. *New Phytologist*, **229**, 2479–2513.

Gilmour, A.R., Cullis, B.R. & Verbyla, A.P. (1997) Accounting for natural and extraneous variation in the analysis of field experiments. *Journal of Agricultural, Biological, and Environmental Statistics*, **2**, 269–293.

GRDC – Grains Research & Development Corporation (2018) Research, Development and Extension Plan 2018-2023: KIT 1.1 Minimise the impact of high temperature at flowering and grain fill on grain yield and stability. Available at: https://rdeplan.grdc.com.au/__data/assets/pdf_file/0020/434090/KIT-1.1_detailed-strategy.pdf [Sourced on 12 September 2021]

Guo, Z., Chen, D., Röder, M.S., Ganal, M.W. & Schnurbusch, T. (2018) Genetic dissection of pre-anthesis sub-phase durations during the reproductive spike development of wheat. *Plant Journal*, **95**, 909–918. https://doi.org/10.1111/tpj.13998

Herrando-Pérez, S., Ferri-Yáñez, F., Monasterio, C., Beukema, W., Gomes, V., Belliure, J. *et al.* (2019) Intraspecific variation in lizard heat tolerance alters estimates of climate impact. *Journal of Animal Ecology*, **88**, 247–257.

Hikosaka, K., Ishikawa, K., Borjigidai, A., Muller, O. & Onoda, Y. (2005) Temperature acclimation of photosynthesis: mechanisms involved in the changes in temperature dependence of photosynthetic rate. *Journal of Experimental Botany*, **57**, 291–302.

Hüve, K., Bichele, I., Tobias, M. & Niinemets, Ü. (2006) Heat sensitivity of photosynthetic electron transport varies during the day due to changes in sugars and osmotic potential. *Plant, Cell & Environment*, **29**, 212–228.

Isbell, R.F. (2002) *The Australian Soil Classification*, Revised edition. Collingwood, Victoria, Australia: CSIRO Publishing.

Kaplan, F., Kopka, J., Haskell, D.W., Zhao, W., Schiller, K.C., Gatzke, N. *et al.* (2004) Exploring the temperature-stress metabolome of Arabidopsis. *Plant Physiology*, **136**, 4159–4168.

Knight, C.A. & Ackerly, D.D. (2002) An ecological and evolutionary analysis of photosynthetic thermotolerance using the temperature-dependent increase in fluorescence. *Oecologia*, **130**, 505–514.

Knight, C.A. & Ackerly, D.D. (2003) Evolution and plasticity of photosynthetic thermal tolerance, specific leaf area and leaf size: congeneric species from desert and coastal environments. *New Phytologist*, **160**, 337–347.

Kotak, S., Larkindale, J., Lee, U., Von Koskull-Doring, P., Vierling, E. & Scharf, K.D. (2007) Complexity of heat stress response in plants. *Current Opinion in Plant Biology*, **10**, 310–316.

Lancaster, L.T. & Humphreys, A.M. (2020) Global variation in the thermal tolerances of plants. *Proceedings of the National Academy of Sciences of the United States of America*, **117**, 13580–13587.

Leon-Garcia, I.V. & Lasso, E. (2019) High heat tolerance in plants from the Andean highlands: Implications for paramos in a warmer world. *PLOS ONE*, **14**, e0224218.

Li, Z., Palmer, W.M., Martin, A.P., Wang, R., Rainsford, F., Jin, Y. *et al.* (2012) High invertase activity in tomato reproductive organs correlates with enhanced sucrose import into, and heat tolerance of, young fruit. *Journal of Experimental Botany*, **63**, 1155–1166.

Lin, Y.-S. (2012) *How will Eucalyptus tree species respond to global climate change?: A comparison of temperature responses of photosynthesis*. Penrith, Australia: University of Western Sydney.

Maechler, M., Rousseeuw, P., Struyf, A., Hubert, M. & Hornik, K. (2021) Cluster: Cluster Analysis Basics and Extensions. *R package version*, **2**(1), 2.

Marias, D.E., Meinzer, F.C. & Still, C. (2017) Leaf age and methodology impact assessments of thermotolerance of *Coffea arabica*. *Trees*, **31**, 1091–1099.

Martineau, J.R., Williams, J.H. & Specht, J.E. (1979) Temperature tolerance in soybeans. II. Evaluation of segregating populations for membrane thermostability. *Crop Science*, **19**, 79–81.

Maxwell, K. & Johnson, G.N. (2000) Chlorophyll fluorescence - a practical guide. *Journal of Experimental Botany*, **51**, 659–668.

Molero, G. & Reynolds, M.P. (2020) Spike photosynthesis measured at high throughput indicates genetic variation independent of flag leaf photosynthesis. *Field Crops Research*, **255**, 107866.

Muggeo, V.M.R. (2003) Estimating regression models with unknown breakpoints. *Statistics in Medicine*, **22**, 3055–3071.

Muggeo, V.M.R. (2008) Segmented: an R package to fit regression models with broken-line relationships. *R News*, **8**, 20–25.

Muggeo, V.M.R. (2016) Testing with a nuisance parameter present only under the alternative: a score-based approach with application to segmented modelling. *Journal of Statistical Computation and Simulation*, **86**, 3059–3067.

Muggeo, V.M.R. (2017) Interval estimation for the breakpoint in segmented regression: a smoothed score-based approach. *Australian & New Zealand Journal of Statistics*, **59**, 311–322.

Nevo, E. (2014) Evolution of wild emmer wheat and crop improvement. *Journal of Systematics and Evolution*, **52**, 673–696.

Oliveira, I.C.M., Guilhen, J.H.S., de Oliveira Ribeiro, P.C., Gezan, S.A., Schaffert, R.E., Simeone, M.L.F. *et al.* (2020) Genotype-by-environment interaction and yield stability analysis of biomass sorghum hybrids using factor analytic models and environmental covariates. *Field Crops Research*, **257**, 107929.

O'Sullivan, O.S., Heskel, M.A., Reich, P.B., Tjoelker, M.G., Weerasinghe, L.K., Penillard, A. *et al.* (2017) Thermal limits of leaf metabolism across biomes. *Global Change Biology*, **23**, 209–223.

Ottaviano, E., Sari Gorla, M., Pè, E. & Frova, C. (1991) Molecular markers (RFLPs and HSPs) for the genetic dissection of thermotolerance in maize. *Theoretical and Applied Genetics*, **81**, 713–719.

Pacifici, M., Foden, W.B., Visconti, P., Watson, J.E.M., Butchart, S.H.M., Kovacs, K.M. *et al.* (2015) Assessing species vulnerability to climate change. *Nature Climate Change*, **5**, 215–224.

Patterson, H.D. & Thompson, R. (1971) Recovery of inter-block information when block sizes are unequal. *Biometrika*, **58**, 545–554.

Perez, T.M. & Feeley, K.J. (2020) Photosynthetic heat tolerances and extreme leaf temperatures. *Functional Ecology*, **34**, 2236–2245.

Porch, T.G. & Hall, A.E. (2013) Heat tolerance. In: Kole, C. & Viswavidyalaya, B.C.K. (Eds.) *Genomics and breeding for climate resilient crops: Vol. 2 target traits*. New York: Springer-Verlag, pp. 167–202.

Posch, B.C., Hammer, J., Atkin, O.K., Bramley, H., Ruan, Y.-L., Trethowan, R. *et al.* (2022) Wheat photosystem II heat tolerance responds dynamically to short and long-term warming. *Journal of Experimental Botany*, **73**(10), 3268–3282.

Posch, B.C., Zhai, D., Coast, O., Scafaro, A.P., Bramley, H., Reich, P.B. *et al.* (2021) Wheat respiratory O_2 consumption falls with night warming alongside greater respiratory CO_2 loss and reduced biomass. *Journal of Experimental Botany*, **73**, 915–926.

Qureshi, M.E., Hanjra, M.A. & Ward, J. (2013) Impact of water scarcity in Australia on global food security in an era of climate change. *Food Policy*, **38**, 136–145.

R-Core-Team. (2021) *R: A language and environment for statistical computing*. Vienna, Austria: R Foundation for Statistical Computing.

Rekika, D., Monneveux, P. & Havaux, M. (1997) The *in vivo* tolerance of photosynthetic membranes to high and low temperatures in cultivated and wild wheats of the *Triticum* and *Aegilops* genera. *Journal of Plant Physiology*, **150**, 734–738.

Ruan, Y.-L. (2014) Sucrose metabolism: Gateway to diverse carbon use and sugar signaling. *Annual Review of Plant Biology*, **65**, 33–67.

Sae-Lim, P., Komen, H., Kause, A. & Mulder, H.A. (2014) Identifying environmental variables explaining genotype-by-environment interaction for body weight of rainbow trout (*Onchorynchus mykiss*): reaction norm and factor analytic models. *Genetics Selection Evolution*, **46**, 16.

Sastry, A. & Barua, D. (2017) Leaf thermotolerance in tropical trees from a seasonally dry climate varies along the slow-fast resource acquisition spectrum. *Scientific Reports*, **7**, 11246.

Schreiber, U. & Berry, J.A. (1977) Heat-induced changes of chlorophyll fluorescence in intact leaves correlated with damage of the photosynthetic apparatus. *Planta*, **136**, 233–238.

Sharma, D.K., Andersen, S.B., Ottosen, C.-O. & Rosenqvist, E. (2012) Phenotyping of wheat cultivars for heat tolerance using chlorophyll a fluorescence. *Functional Plant Biology*, **39**, 936–947.

Sharma, D.K., Torp, A.M., Rosenqvist, E., Ottosen, C.-O. & Andersen, S.B. (2017) QTLs and potential candidate genes for heat stress tolerance identified from the mapping populations specifically segregating for F_v/F_m in wheat. *Frontiers in Plant Science*, **8**, 1668.

Shen, S., Ma, S., Chen, X.-M., Yi, F., Li, B.-B., Liang, X.-G. *et al.* (2022) A transcriptional landscape underlying sugar import for grain set in maize. *The Plant Journal*, **110**, 228–242.

Silva-Pérez, V., De Faveri, J., Molero, G., Deery, D.M., Condon, A.G., Reynolds, M.P. *et al.* (2020) Genetic variation for photosynthetic capacity and efficiency in spring wheat. *Journal of Experimental Botany*, **71**, 2299–2311.

Slowikowski, K. (2021). ggrepel: Automatically position non-overlapping text labels with 'ggplot2'. R package version 0.9.1. https://CRAN.R-project.org/package=ggrepel.

Smith, A., Cullis, B. & Thompson, R. (2001) Analyzing variety by environment data using multiplicative mixed models and adjustments for spatial field trend. *Biometrics*, **57**, 1138–1147.

Smith, A.B. & Cullis, B.R. (2018) Plant breeding selection tools built on factor analytic mixed models for multi-environment trial data. *Euphytica*, **214**, 143.

Smith, A.B., Ganesalingam, A., Kuchel, H. & Cullis, B.R. (2015) Factor analytic mixed models for the provision of grower information from national crop variety testing programs. *Theoretical and Applied Genetics*, **128**, 55–72.

Sunday, J.M., Bates, A.E. & Dulvy, N.K. (2011) Global analysis of thermal tolerance and latitude in ectotherms. *Proceedings of the Royal Society B: Biological Sciences*, **278**, 1823–1830.

Theis, J. & Schroda, M. (2016) Revisiting the photosystem II repair cycle. *Plant Signaling & Behavior*, **11**, e1218587.

Trethowan, R., Chatrath, R., Tiwari, R., Kumar, S., Saharan, M.S., Bains, N. *et al.* (2018) An analysis of wheat yield and adaptation in India. *Field Crops Research*, **219**, 192–213.

Trethowan, R.M. (2022) Abiotic stresses. In: Reynolds, M.P. & Braun, H.-J. (Eds.) *Wheat Improvement: Food Security in a Changing Climate*. Springer Nature: Switzerland, pp. 159–176.

Ullah, S., Bramley, H., Daetwyler, H.D., He, S., Thistlethwaite, R. & Trethowan, R. (2018) Genetic variation in emmer wheat (*Triticum dicoccon* Schrank) improves the heat tolerance of bread wheat. *Frontiers in Plant Science*, **9**, 1529.

Vierling, E. (1991) The roles of heat shock proteins in plants. *Annual Review of Plant Physiology and Plant Molecular Biology*, **42**, 579–620.

Weng, J.-H. & Lai, M.-F. (2005) Estimating heat tolerance among plant species by two chlorophyll fluorescence parameters. *Photosynthetica*, **43**, 439–444.

Wickham, H. (2007) Reshaping Data with the reshape Package. *Journal of Statistical Software*, **21**, 1–20.

Wickham, H. (2016) *ggplot2: Elegant Graphics for Data Analysis*, 2nd/Ed. edition. New York: Springer-Verlag.

Wright, I.J., Reich, P.B., Atkin, O.K., Lusk, C.H., Tjoelker, M.G. & Westoby, M. (2006) Irradiance, temperature and rainfall influence leaf dark respiration in woody plants: evidence from comparisons across 20 sites. *New Phytologist*, **169**, 309–319.

Wright, I.J., Reich, P.B., Cornelissen, J.H.C., Falster, D.S., Garnier, E., Hikosaka, K. *et al.* (2005) Assessing the generality of global leaf trait relationships. *New Phytologist*, **166**, 485–496.

Yoshioka-Nishimura, M. (2016) Close relationships between the PSII repair cycle and thylakoid membrane dynamics. *Plant and Cell Physiology*, **57**, 1115–1122.

Zadoks, J.C., Chang, T.T. & Konzak, C.F. (1974) A decimal code for the growth stages of cereals. *Weed Research*, **14**, 415–421.

Zhao, C., Liu, B., Piao, S., Wang, X., Lobell, D.B., Huang, Y. *et al.* (2017) Temperature increase reduces global yields of major crops in four independent estimates. *Proceedings of the National Academy of Sciences of the United States of America*, **114**, 9326–9331.

Zhu, L., Bloomfield, K.J., Hocart, C.H., Egerton, J.J.G., O'Sullivan, O.S., Penillard, A. *et al.* (2018) Plasticity of photosynthetic heat tolerance in plants adapted to thermally contrasting biomes. *Plant, Cell & Environment*, **41**, 1251–1262.